5-2017

Novel device for improved diagnosis and monitoring of rotator cuff injury

Brittany Nicole Hall
Clemson University, bnhall@clemson.edu

NOVEL DEVICE FOR IMPROVED DIAGNOSIS AND MONITORING OF ROTATOR CUFF INJURY

A Thesis
Presented to
the Graduate School of
Clemson University

In Partial Fulfillment
of the Requirements for the Degree
Master of Science
Bioengineering

---

by
Brittany Nicole Hall
August 2014

Accepted by:
Dr. David Kwartowitz, Committee Chair
Dr. Charles Thigpen
Dr. Delphine Dean

ABSTRACT

Rotator cuff disease impacts approximately over 50% of the population above the age of 60, causing pain and ultimately possible loss of shoulder function. The rotator cuff is composed of muscles and tendons that work in tandem to support the shoulder and aid in the movement of the arm. History of trauma and increased age can lead to a rotator cuff tear, which can range in severity from a partial-thickness tear to a full-thickness, total rupture. Currently, diagnostic techniques for rotator cuff disease are based on physical assessment, detailed patient history, and medical imaging, primarily X-ray, MRI and ultrasonography. However, limitations still exist regarding rotator cuff diagnosis and monitoring. Ultrasound has been shown to have good accuracy in the identification and measurement of full-thickness and partial-thickness rotator cuff tears. Quantitative data regarding rotator cuff tears is not as readily available as the qualitative data provided by the aforementioned techniques. The device designed through this study improves the method of transduction and the analysis of in situ measurement of rotator cuff biomechanics. Improvements include the ability of the clinician to apply a uniform force to the underlying musculotendentious tissues while simultaneously obtaining an ultrasound image and the addition of Bluetooth for ease of data transfer. Preliminary studies were performed with the device on both post-operative and healthy patients, in which the stress and strain experienced by the rotator cuff tissue was analyzed. This device will ultimately aid in developing a more thorough predictive diagnostic model for the treatment of rotator cuff disease and aid clinicians in choosing the best treatment option for patients.

ACKNOWLEDGMENTS

I would like to thank, first and foremost, my committee chair, David Kwartowitz, for allowing me the opportunity to work on this project and providing me with guidance throughout it. I would also like to thank my other committee members Chuck Thigpen and Delphine Dean for providing constant assistance and guidance. I would also like to say a big thank you to Anup Pillai as well as the rest of the CUTTERS lab members . I would also like to thank my parents for supporting and encouraging me throughout the past year during my Master's studies and research. Lastly, I would like to thank my friends for their support and encouragement. I would also like to the SCMedTrans Tech funding for financial assistance.

TABLE OF CONTENTS

Page

LIST OF TABLES

LIST OF FIGURES

List of Tables (Continued)

Figure Page

CHAPTER ONE

INTRODUCTION

Overview

Rotator cuff disease is the most common shoulder problem, with about 20.7-22.1% being affected by it. [1,2] The largest risk factors for rotator cuff tears include a history of trauma and a person's age. [1] The number of those affected by the disease increases with age; over 50% of the population over the age of 60 is affected by rotator cuff disease.[1, 3, 4] Rotator cuff tears have significant impacts on a patient's life aside from the pain experienced by the disease, which can ultimately cause loss of function. The impacts include significant decrease in overall health, particularly with regards to physical functioning, social functioning, physical health, and emotional health. [5,6] It has even been suggested that a patient's quality of life is effected to the same degree as those with one of five major medical conditions: hypertension, congestive heart failure, acute myocardial infarction, diabetes mellitus and clinical depression. [5] Although tears are common in the elderly, they can occur in those under the age of 40 if accompanied by acute trauma. [7] Of all the patients seen by shoulder surgeons, rotator cuff injuries account for 30%. [8,9]

Anatomy

The shoulder joint, or glenohumeral joint, is a ball and socket joint that allows for interaction between the glenoid fossa of the scapula and the head of the humerus, which is shown in figure 1.1. [10] This joint is the most mobile joint in the body whose main purpose is the correct functional placement of the hand. [8,11] This task requires mobility, strength, and stability. The

rotator cuff is comprised of four main muscles and their musculotendinous attachments, which provide the stability of the glenohumeral joint. [8,12]

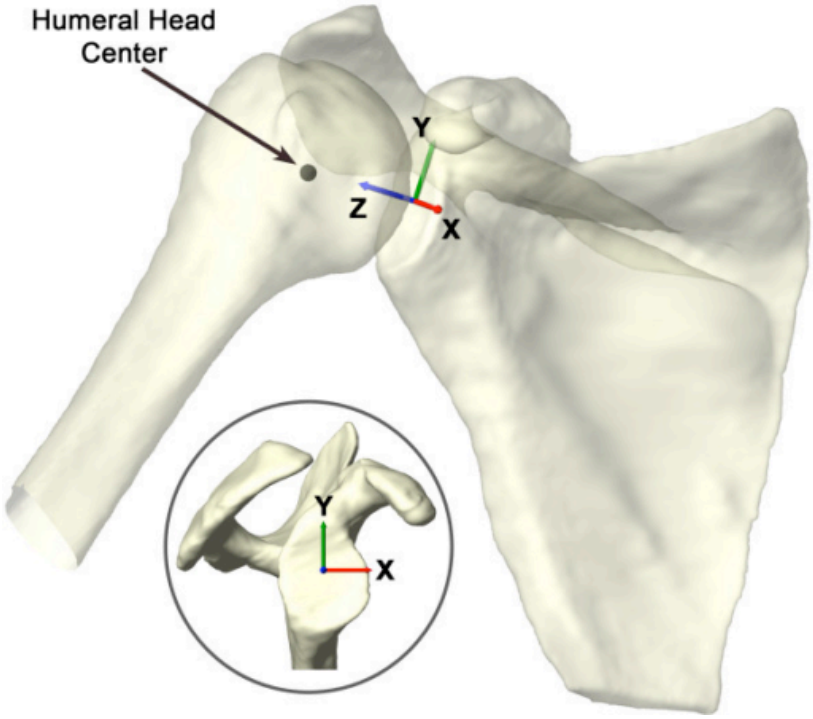

Figure 1.1: Glenohumeral Joint Surface Model

The rotator cuff is comprised of four main muscles: the subscapularis, the supraspinatus, the infraspinatus, and the teres minor, as shown in figure 1.2 and 1.3. [13] The subscapularis muscle originates in the scapula and is innervated by the subscapular nerve. [12] It is a large structure that is flat in shape and is powerful enough to oppose the function of both the infraspinatus and teres minor muscles posteriorly. [14] The supraspinatus originates in the scapula and inserts into the greater tuberosity via its tendon. [12] It works in conjunction with the teres minor, which originates in the scapula as well. The teres minor is innervated by the axillary nerve and inserts into the greater tuberosity. The infraspinatus originates in the supraspinous

fossa and is innervated by the suprascapular nerve. All of the aforementioned muscles end in tendons that fuse with the fibrous capsule to form the cuff. [14]

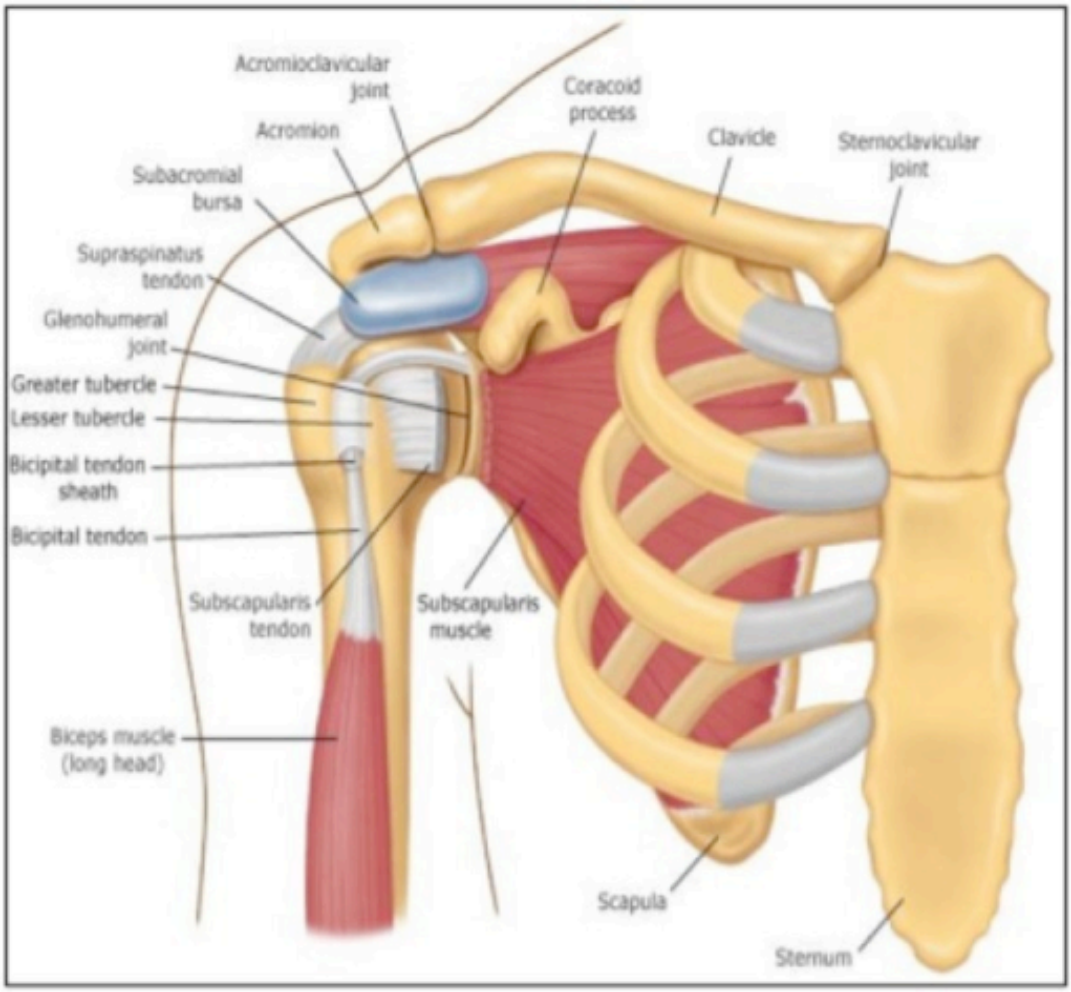

Fig 1.2: Anterior View, Rotator Cuff Anatomy

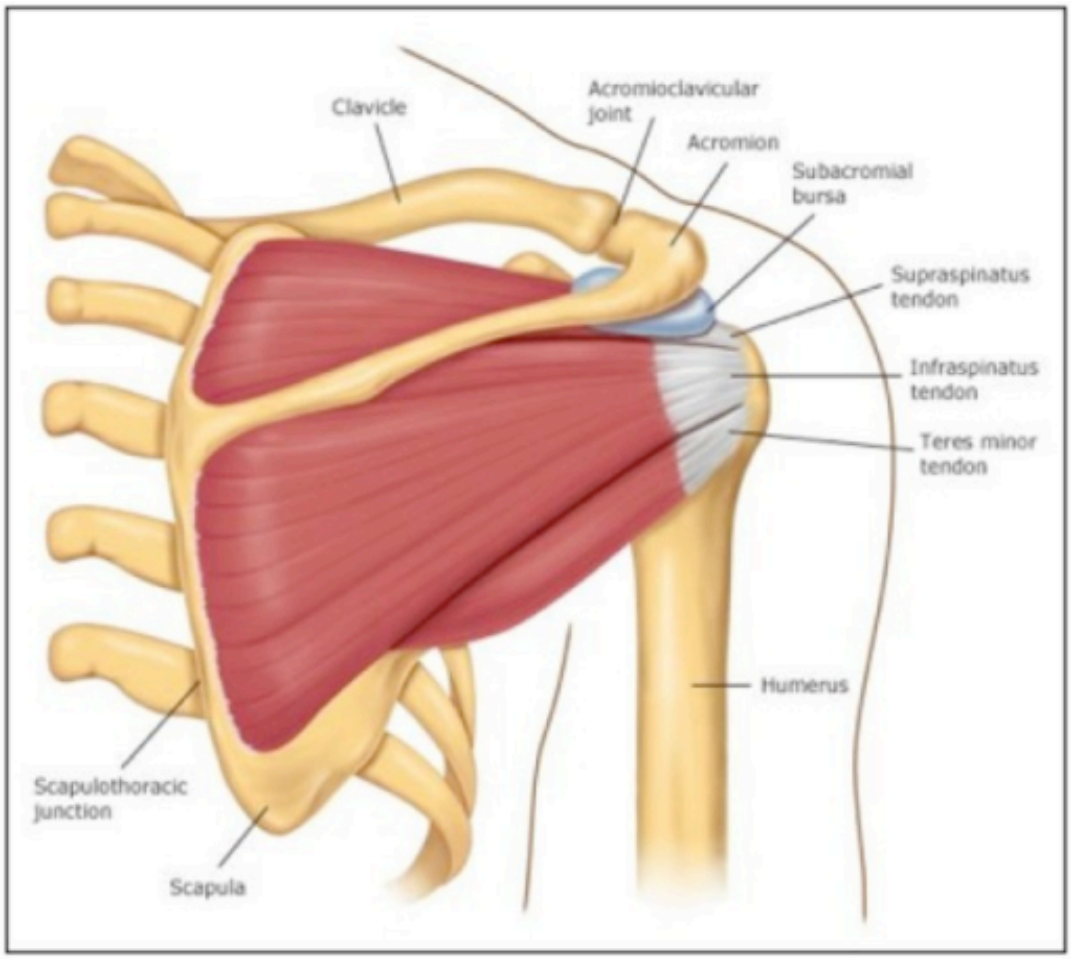

Fig 1.3: Posterior View, Rotator Cuff Anatomy

During shoulder motion, the muscles of the rotator cuff stabilize the glenohumeral joint. Contraction of the supraspinatus in conjunction with the deltoid muscle is responsible for abduction of the arm.[8,15] Supraspinatus activity continues throughout the process of abduction.[15] This upward motion caused by the supraspinatus is opposed by the action of the infraspinatus, subscapularis, and teres minor, which all depress the humeral head to ensure and maintain stability of the joint.[8] The muscles of the rotator cuff have varying contributions to the torque produced during abduction, with 30% being due to the subscapularis, 25% by the supraspinatus, and 10% by the infraspinatus.[16] The four muscles of the rotator cuff both generate torque and

depress the humeral head, allowing for stabilization of the joint. In large rotator cuff tears, this stabilization is compromised and the humeral head is allowed to migrate. [12]

Rotator Cuff Tears

Typically, a rotator cuff tear is the result of degeneration, as a result of shear wear in the presence of hypovascularity that reduces tendon integrity. [11] An extreme overload event, such as a significant fall, motor vehicle crash, or shoulder dislocation, can also cause a tear. [8,11] However, degeneration is most frequently the cause of tears as opposed to trauma. [8] The three stages of rotator cuff disease defined by Neer depict the anatomical changes within the rotator cuff that lead to the varying degrees of thickness: Stage I tears occur in patients younger than 25 and are typically due to edema and hemorrhage of the bursa and tendon; Stage II tears occur in patients 25-40 years old and are typically due to tendonitis and fibrosis; Stage III tears occur in individuals over the age of 40 and involves partial or full-thickness tearing of the cuff. [17]

A study of cadaveric models found that of 30.24% of tears found, 11.75% were full-thickness and 18.49% were partial-thickness. [18] In an autopsy study, the incidence of partial tears was found to be 28.7%. [19] In smaller tears, increased fibroblast cellularity, increased expression of leucocytes, and increased expression of vascular markers occur, all which are indicative of inflammation and healing. However, these traits are seen less often as the size of the tear increases. [20] In large tears, evidence of edema and degeneration has been seen with little signs of inflammation and healing, as seen in smaller tears. This suggests that smaller tears have a greater chance of healing than larger ones due to the presence of anatomical markers associated with inflammation and healing. [20] It has been demonstrated that 10% of partial-thickness tears fully heal and 10% will become smaller. However, 53% of partial-thickness tears will propagate, with

28% progressing to full-thickness tears.[21] When the progression to a full-thickness tear occurs, persistent tendon defect can occur if surgical measures are not taken, which can ultimately lead to detrimental effects in both cells and tissue within the joint.[9] It has been suggested that supraspinatus involvement always occurs in rotator cuff ruptures.[19] The supraspinatus tendon becomes thickened and more likely to tear with increasing age.[22]

The most common symptoms associated with rotator cuff disease are pain in the shoulder, moderate to severe weakness, and reduced range of motion.[23] Although some rotator cuff injuries present debilitating symptoms that significantly alter the quality of life, symptoms are not always present with the existence of a tear.[2] Only 34.7% of rotator cuff tears are associated with symptoms, leaving 65.3% of rotator cuff tears to be asymptomatic.[2] The presence of asymptomatic tears is common, and increases in probability with age.[2,23-25] Asymptomatic tears constitute for about half of the tears in people in their 50s and over two-thirds of those in people over the age of 60.[2] Over half of asymptomatic rotator cuff tears have been demonstrated to progress to symptomatic in less than three years, during which the tear increases in size.[25] Overall, asymptomatic tears are twice as likely as symptomatic tears within the population.[2]

Across literature, it is unanimously agreed upon that the likelihood of rotator cuff disease increases with age.[1,2,4,19,23,24,26] Approximately 30-54% of individuals over the age of 60 experience the pain and debilitation associated with rotator cuff disease.[4,24,26] The prevalence increases markedly above the age of 80 in which 36.6%-80% of individuals are affected by rotator cuff disease.[2,4] This prevalence significantly increases every decade, affecting 10.7% of those in their 50s, 15.2% of those in their 60s, 26.5% of those in their 70s, and 36.6% of those in

their 80s, in a particular study. [2] It has been suggested that neither dominance nor gender have any affect on rotator cuff disease. [4]

Although rare, rotator cuff disease can occur in individuals under the age of 40. The prevalence of rotator cuff tears under the age of 40 is 0-4%. [2,24] This is typically due to acute trauma caused by impingement and flexibility deficits, strength deficits, or both. [7] This type of injury is often seen in throwing athletes such as baseball players, rowers, and tennis players.

When torn, it has been observed that increasing rotator cuff tear thickness is correlated with increased strain in the intact posterior portion and decreased strain in the torn anterior portion. [27] The stiffness of a torn supraspinatus initially decreases, but quickly increases with time from the injury, as observed in animal studies where rotator cuff tendons were torn and observed. [28] The presence of atrophy and fatty infiltration in rotator cuff tears directly correlates with how repairable a tear is. It has been observed that fatty infiltration and atrophy increase within a 48-month period and within one year of rotator cuff tendon repair, atrophy improves partially while fatty infiltration does not recover. [29,30]

With regards to medical costs, workers compensation, and decreased productivity, it has been suggested that rotator cuff disease accounts for $3-5 billion a year. [31,32] Second to back pain, rotator cuff injuries are one of the main cases of lost work time in manual laborers. [33] Rotator cuff tendonitis is common among those who work in heavy labor-intensive fields. For example, approximately 18.3% of shipyard welders and 16.2% of plate workers experience the pain associated with rotator cuff disease, which has been attributed to the heavy hand tool use in such fields. This excessive muscle maneuver increases strain in the supraspinatus and the infraspinatus. This strain on the supraspinatus that occurs in overhead lifting significantly contributes to the shoulder disabilities often seen in individuals in theses professions. [33]

Existing Diagnostic Methods

Currently the diagnosis of rotator cuff disease includes patient history analysis, pain assessment, a physical examination, and testing utilizing imaging modalities. During the physical examination, a physician assesses for signs of impingement, which includes applying various forces, varying from 5-10 pounds, to the joint at varying angles as well as analyzing the range of motion. Force is applied during downward pushes to examine if pain exists at this point and disappears when the force and push is removed, shown in figure 1.4. [34] With rotator cuff disease, pain is often exacerbated with overhead movements, which is another symptom clinicians look for during the physical examination. [12] Although patient history and a physical examination are often the first steps performed during rotator cuff diagnosis, it has been suggested that there is a lack of a clinically relevant diagnosis utilizing the two. [35] If the physical examination, pain assessment, and patient history point towards a positive diagnosis, imaging modalities are utilized to further differentially diagnose the injury.

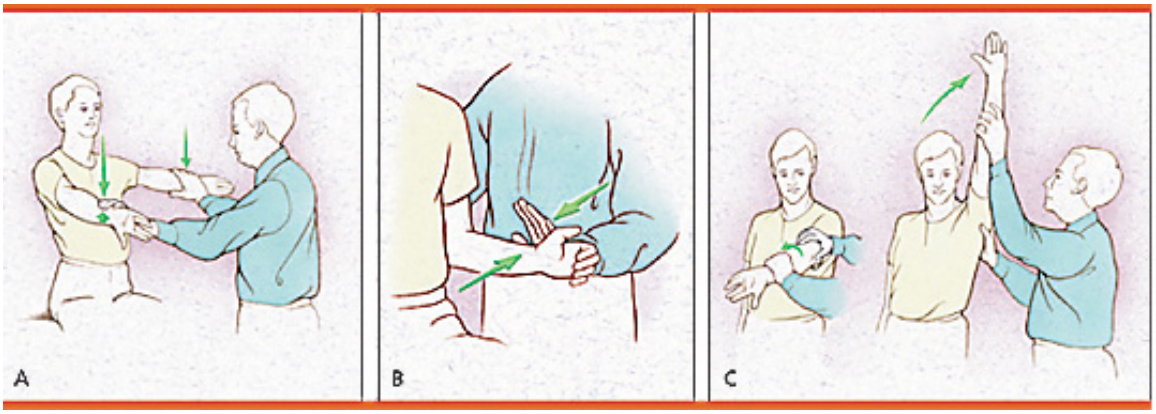

Figure 1.4: Rotator Cuff Physical Examination

Magnetic resonance imaging (MRI) is often used in the diagnosis of rotator cuff injuries for patients considering surgery. MRI has excellent soft tissue contrast and does not use ionizing radiation, making it a good candidate for the diagnosis of injuries in the shoulder joint. [36] This technique not only limits the analysis of real-time results, but is also costly, time-consuming, and requires a large space for the equipment. It is the high-cost and time consumption associated with MRI that often makes it an impractical diagnostic device for rotator cuff injuries. [22] It has also been observed that MRI does not have the ability to differentiate between partial and full-thickness tears nor incomplete tears. This modality also does not have the ability to differentiate between the different surfaces at which a tear is located. [37]

The other imaging modality used in the diagnosis of rotator cuff tears is ultrasound. Ultrasound is an attractive diagnostic device for several reasons. Obtaining images with ultrasound is a relatively quick process that is safe and noninvasive. It is also not limited by patient size, cooperation, or positioning and can be used bedside. It is also readily available. [38] Ultrasound allows for real-time results and has been suggested to be a reliable, timesaving practice in the diagnosis of rotator cuff tears when performed by a skilled clinician. [39] Studies have reported varying sensitivity and specificity values for ultrasound, ranging from 96.2-100% and 95.4-97%, respectively, for full-thickness tears. [39,40] The estimation of tear size is more accurate for larger tears than smaller tears with ultrasound, with 96.5% of larger tears being correctly estimated and 91.6% of smaller tears being correctly estimated. [39] When used to diagnose partial-thickness and full-thickness tears, ultrasound detects 80% and 90%, respectively, of total tears, correctly showing the site of the tear in every patient. [41]

In the argument of whether ultrasound or MRI is the best diagnostic modality for rotator cuff disease, various data and opinions exist. Some argue that ultrasound is not as accurate as

MRI in the diagnosis of rotator cuff tears. [42] However, many studies suggest that ultrasound and MRI are comparable for the diagnosis of rotator cuff disease, and are essentially equal diagnostic tools. [43-45] It has also been observed that the sensitivity of ultrasound diagnosis (93.4%) is greater than MRI diagnosis (87.5%). [46] Due to the fact that ultrasound has a high sensitivity and specificity, is economic, and fast, it is the preferred diagnostic method. [45,46] Ultrasound also performs better in the detection of partial-thickness tears. [47]

Current Diagnostic Limitations

Although the aforementioned methods have the ability to correctly diagnose rotator cuff disease, there is a lack of thorough, biomechanical data with each method. Although qualitative data is available, limitations exist with the aforementioned tests that prevent clinicians from obtaining both qualitative and quantitative data to aid in the diagnosis. This indirect assessment also prevents diagnoses from being standardized. Various clinicians interpret the qualitative data differently provided by the techniques currently used, causing diagnoses to be very subjective. In short, there is little scientific basis upon which treatment decisions are currently made. [38] The availability of a quantified standardized procedure would allow for a complete and accurate comparison of tears between various patients as well as tears before and after treatment or surgery in the same patient. The ability to quantify rotator cuff tears is something that can overcome the limitations currently encountered. [38]

As previously stated, little research has been performed in the area of quantifying the active rotator cuff tendon. However, interest in this area is developing due to the relatively high rate of failed rotator cuff repairs. [38] Bull, Reilly, et al described the use of arthroscopically insertable force probes to study the rotator cuff in vivo. [48,49] These force sensors were

arthroscopically implanted into the subscapularis tendon, after which forces were applied during active tendon movement and measured. The results of the subscapularis tendon loading suggested that the subscapularis is capable of producing up to 250 N of force during maximum internal rotation of the shoulder. [48] Kim et al also described an in vivo supraspinatus analysis which documented the strain of the superficial, middle, and deep regions of the supraspinatus tendon. [50] The displacement and strain was measured during isotonic and isometric shoulder movement, in which a greater displacement was observed in the superficial region than the deep region during isometric motion, 1.66mm and 0.61mm respectively. During isotonic motion, the displacement was greater in the deep region than the superficial region, 1.61mm and 0.70mm respectively. [50]

Studies have been performed using an ultrasound in vivo approach on the Achilles tendon [51-53], tibialis anterior tendon [54,55], and patellar tendon. [56,57] However, such an approach has not been extensively studied in the rotator cuff. The measurement of in vivo tendon function via ultrasound utilization is a method that shows great promise for the rotator cuff tendon, especially when combined with force and stress deformation estimations. [38] Tendon stiffness can be a predicative model for rotator cuff disease and can be measured through ultrasound utilization due to the fact that ultrasound can obtain images before, during, and after compression of the tendon. Therefore, tissue strain can be measured utilizing the ultrasound probe to administer force. [58] This force will allow for the collection of quantitative data that can then be paired with the qualitative data obtained from ultrasound imaging to produce a more thorough, comprehensive diagnosis of rotator cuff injury. With this method, force sensors do not have to be physical implanted, there are no known side effects, and real-time, dynamic images can be obtained and paired with quantitative data. This will allow for a more objective judgment of postoperative

rotator cuff healing through mechanical data that is currently not available. This will also allow the use of tendon biomechanics to serve as an indicator of normal versus compromised tendon function, allowing for a standardized diagnosis to exist among clinicians regarding rotator cuff disease. In this study, an apparatus was developed that utilizes force measurements and ultrasound images to obtain, compile, and process raw data to yield diagnostically relevant data indicative of rotator cuff tendon mechanics. This device was then tested on patients with normal and compromised rotator cuff tendons to obtain preliminary diagnostic data regarding force measurements relating to rotator cuff disease.

CHAPTER TWO

DEVICE DESIGN AND SOFTWARE

Device Design

The original idea for the device was to have a moving component that allowed for the measurement of a baseline force and compression force, ergonomic. Earlier iterations of this device that were designed were too bulky to allow for the incorporation of the force sensors while also being adaptable to different types of ultrasound probes. Due to the requirement that the device needed to fit a variety of ultrasound probes, the smallest component of the device needed to be big enough to fit the largest, most common probe, the HFL50x 15-6 MHz transducer. Hence, the final iteration of the device was created and is comprised of two parts, an internal component and a shell.

The internal piece has two parts that fit together, as shown in figure 2.1. These two parts are attached onto an ultrasound probe that is pushed into the patient's shoulder and, therefore, rotator cuff tissue. This part is what is utilized, in conjunction with the ultrasound probe, to administer the force that is measured and reported. The internal piece is designed to be universal for all ultrasound probes, which is achieved by having several different options of the internal piece. All of these pieces have the same exterior design, so that they are all compatible with the same shell, with various foam patterns on the interior to compensate for the different probe sizes available on the market. The transducer is placed within the long axis of the infraspinatus muscle at the level of the posterior glenohumeral joint line, inferior to the spine of the scapula. Each ultrasound image is centered along the spinoglenoid notch, where standardized measurements are calculated.

The shell, which is shown in figure 2.2, is comprised of two parts. The cross-section of the shell, which is one of the two pieces, is shown in figure 2.3. Two force sensors are placed on the bottom of these parts, which then attach over the internal component, as shown in figure 2.4. Therefore, when fully assembled, the shell contains force sensors that push against the internal component when applied to rotator cuff tissue, as shown in figure 2.5. This allows for the sensors to read the force applied to the tissue by the clinician. The top of the shell was designed with a curved surface to fit the contour of the human hand, making the use of this device more comfortable for the end user. This curvature also allows the device to be fully functional with the use of only one hand, much like the use of an ultrasound probe. This aspect of the device mitigates a learning curve with the end user, due to the fact that its handling and use is much like that of the ultrasound probe itself.

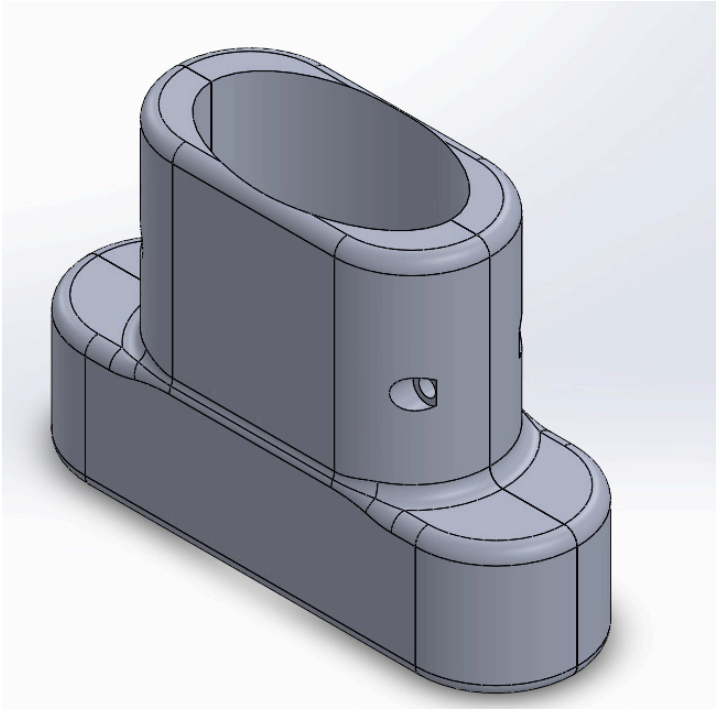

Figure 2.1: Internal Component of the Device

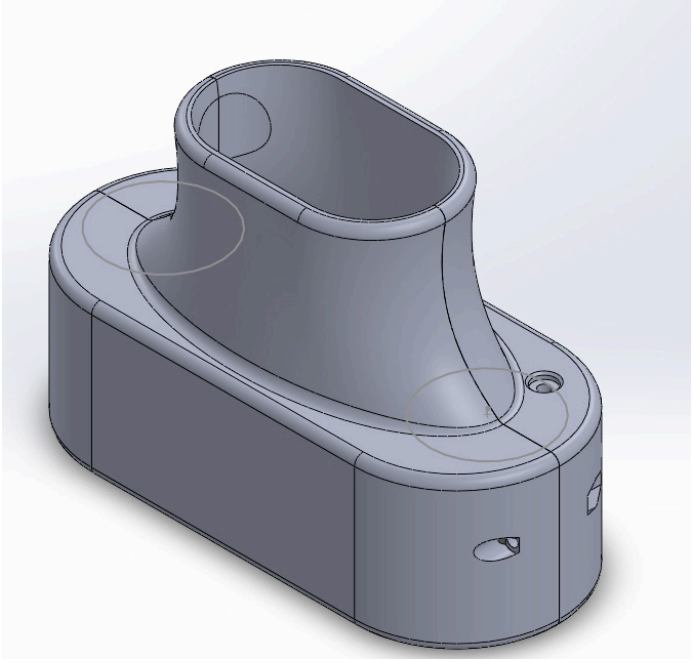

Figure 2.2: Shell of the Device

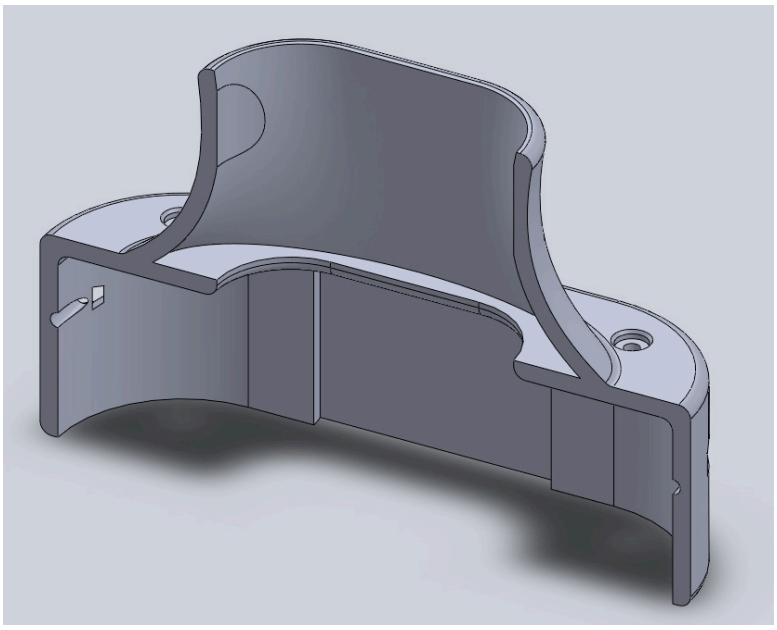

Figure 2.3: Cross-section of the Shell of the Device

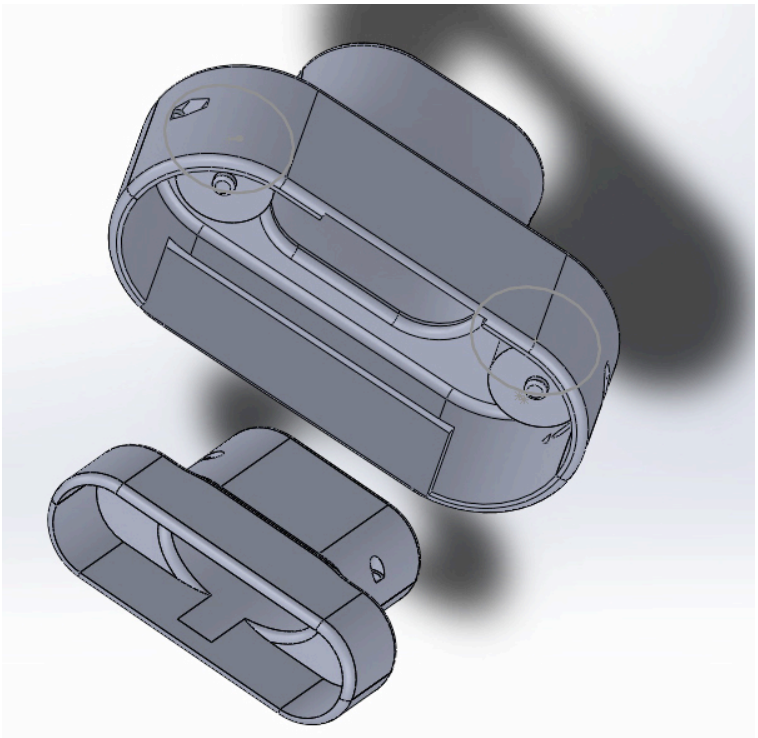

Figure 2.4: Full Device with Separated Components

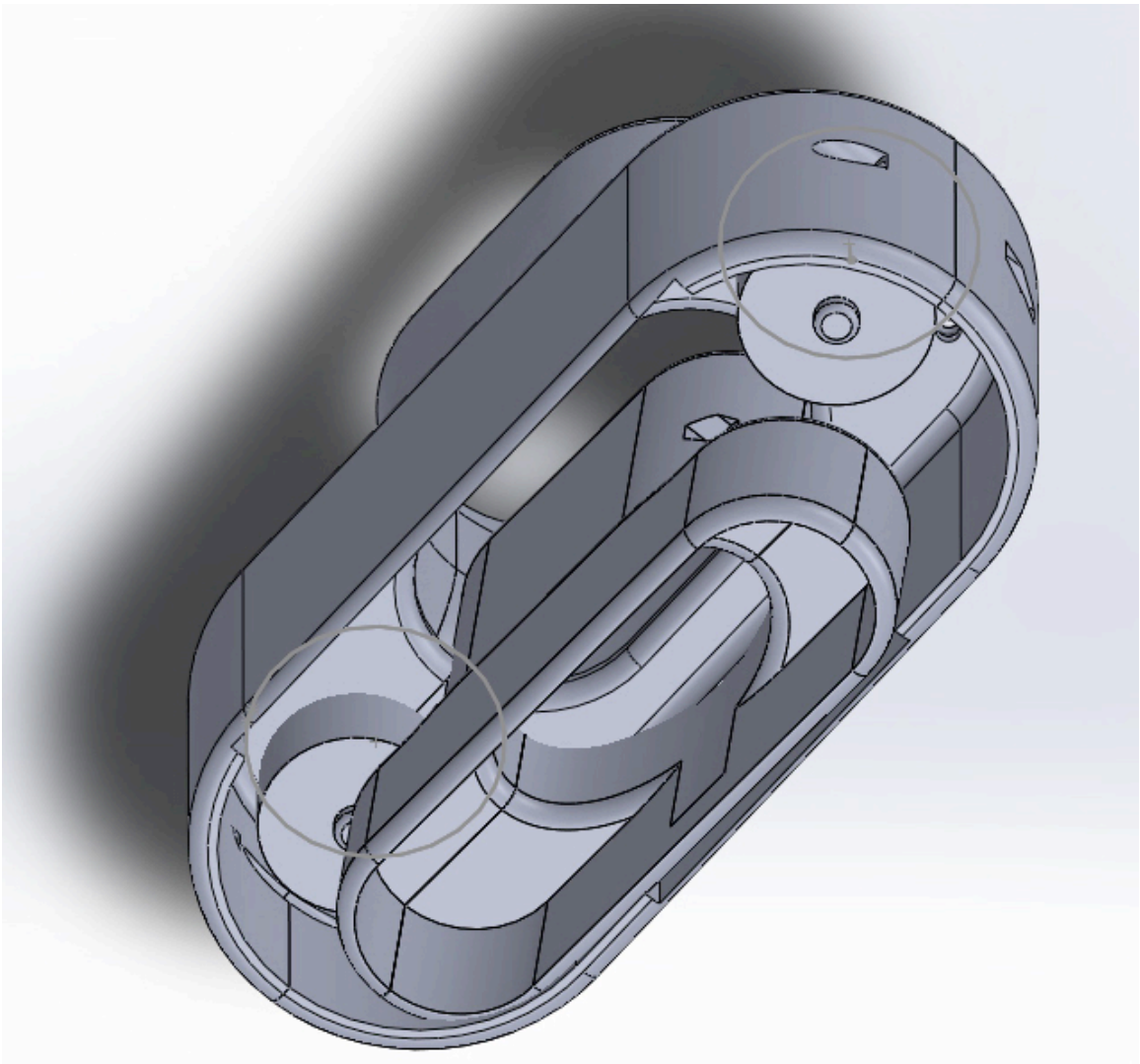

Figure 2.5: Fully Assembled Device

This design is more ergonomic and reliable as compared to the first iteration[54]. The first iteration of the apparatus had some drawbacks, the most significant being the force measurements from the sensor were not uniform. The old iteration used flex sensor to measure force, which is a less reliable way of measuring force than the compression load cell sensors used in this device. Also, the flex sensors have a shorter life span than those used in this device and are more prone to wear. This led to the clinician having to

repeat the procedure several times to obtain acceptable readings. The improved device also incorporates the hardware of the device, the battery and Arduino board, within the device, whereas the old device had a box external to the device itself containing the hardware. The Fio V3 Arduino board used in this device is also much smaller in size than the Arduino Uno board used in the old device. The previous iteration also utilized springs, which are susceptible to wear and corrosion. This improved device is comprised of two parts, where one part is able to move over the other. This aspect decreases the likelihood of the wear and tear that existed with the previous iteration. The large springs in the previous device design also required the use of both hands to compress the device, and allow for the compression force measurement. This meant that the device was not held like the ultrasound probe itself, and created a learning curve for the clinician using it. The new design is smaller and only requires one hand for use and is gripped in a similar manner as an ultrasound probe.

Software and Functioning

The system within the device allows for the measurement of force measurements, both at a baseline value and a compression value, after which the difference is analyzed. The system does the following: (i) obtains both baseline and force measurements when attached to the probe that is used to push into the tissue; (ii) difference between the baseline and force is calculated then utilized to obtain stress; (iii) the length of the tissue at the baseline and compression force are measured on ultrasound images; (iv) the

difference in length between the baseline and force lengths is calculated and utilized to obtain strain; and (v) Young's Modulus is calculated using the calculated stress and strain. This process is outlined in Figure 2.6.

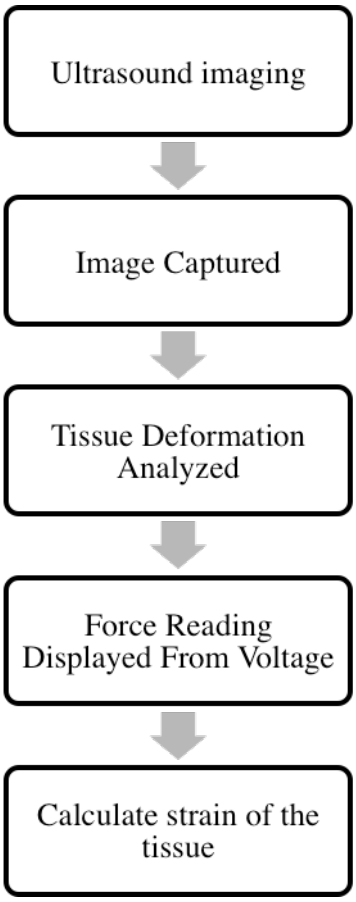

Figure 2.6: Procedural Block Diagram

Step i listed above can further be explained with respect to how the device allows for the force measurement to be obtained and read. This is displayed in Figure 2.7. First, two compression load cells force transducers collect the data. When the device is used, these sensors, which are attached to the shell, push onto the exterior surface of the

internal piece. The sensors report the voltage associated with the amount of force the clinician applies with the aid of the transducer to the patients shoulder.

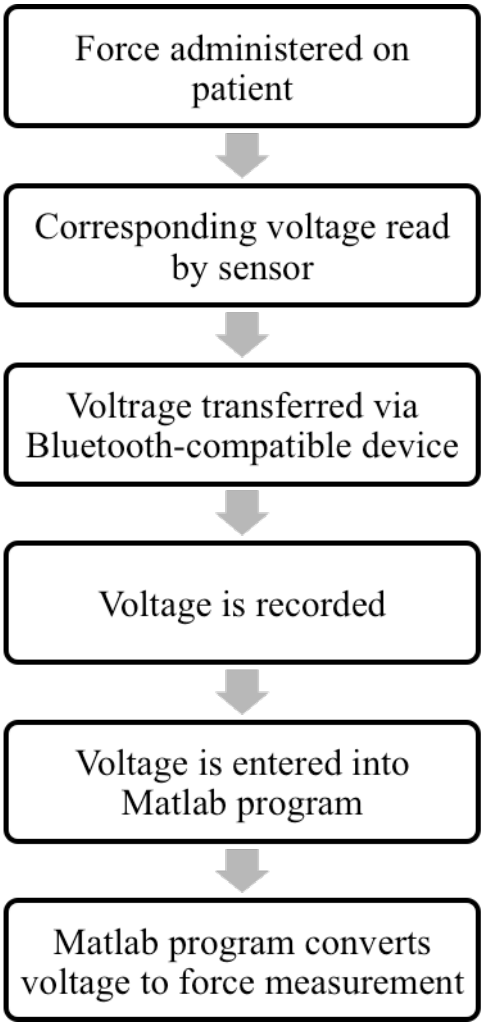

Figure 2.7: Software Procedural Diagram

The obtained voltages are then transferred to a laptop via the Bluetooth present on the Fio V3 Arduino board fitted on the device [59]. The previous iteration of this device used an USB cable to transfer the obtained measurement to a computer, which is something that needed to be improved upon. With respect to the earlier iteration,

clinicians complained about the how difficult it was to use a device that was hooked up to a computer via a cable along with the transducer that the device surrounds also being hooked up to a separate system. This prevented ease of use, and it was essentially a nuisance for clinicians to try to use a device wired to several different machines. Therefore, with this device, Bluetooth was incorporated into the hardware to prevent this annoyance and allow the clinician to use the device more easily. With the Bluetooth, the device is free of cables, and does not have to be attached to a computer. The laptop that displays the collected data can be placed anywhere in the near vicinity, allowing the clinician to used the improved device almost like an ultrasound transducer.

After the recorded voltage is transferred to a laptop, it is entered into a Matlab program that was created to convert the voltage to the corresponding force measurement. Once the sensors were incorporated into the device, calibrations were performed to obtain the forces that correspond to the voltages read by the sensors. Various weights were loaded onto the device and the corresponding output voltages were recorded. For each weight, two voltages were recorded, one for each of the sensors. Several trials were performed, and the voltages for each weight were averaged as well as for the two sensors. A linear interpolation was then performed to ensure each possible voltage output had a corresponding force measurement. A look-up table was created with all possible voltage outputs and the corresponding force measurements, which was incorporated into a Matlab program that allows the clinician to enter the voltage displayed from the device to obtain the correct force measurement. Ultimately, this program takes the voltage input and gives

the corresponding calibrated force using the look up table. If the voltage entered is not available in the table, the program interpolates linearly to find the corresponding force.

CHAPTER THREE

PATIENT DATA

Methods

A clinical study was performed to ensure the proper functioning of the device as well as to obtain preliminary results. The device was used on a total of eight patients, four healthy patients and four post-operative patients. The post-operative patients had rotator cuff repairs performed approximately two years prior to testing. The healthy patients were in their mid-20s and had no previous rotator cuff or shoulder injuries. For the post-operative patients, three trials of both the involved, the shoulder the surgery was performed on, and non-involved shoulder were performed. For the healthy patients, three trials of both the dominant and non-dominant shoulder were performed.

For each trial, the device was attached at a Sonosite HFL50 transducer and attached to a Sonosite ultrasound system. The device was then used to obtain a baseline image and the corresponding force measurement, which was done by gently touching the probe to the patient's skin. The clinician then applied as much force as possible to the tendon and a force measurement was recorded while simultaneously obtaining an ultrasound image. OsiriX was then used to measure the length of the tendon in both the baseline and force images for each trial, as shown in figures 3.1 and 3.2. The strain was calculated by dividing the difference between the baseline and force lengths (Δl) by the baseline length (l). Stress was calculated by dividing the difference of the baseline and compression force measurements by the area of the transducer. The stress and strain

relationship, Young's modulus, was then plotted. Stiffness was also calculated, difference in force measurements divided by the difference in lengths (displacement), and plotted.

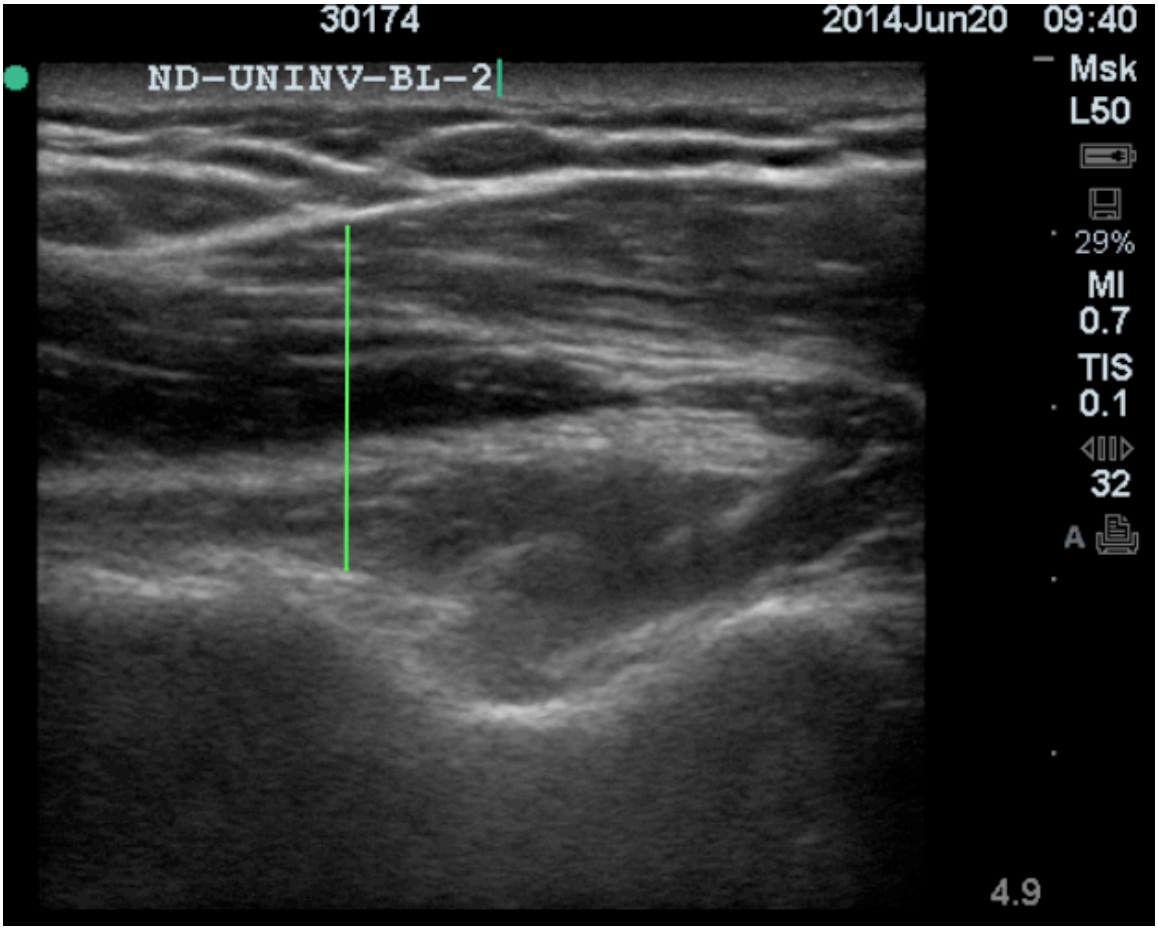

Figure 3.1: Baseline length measurement

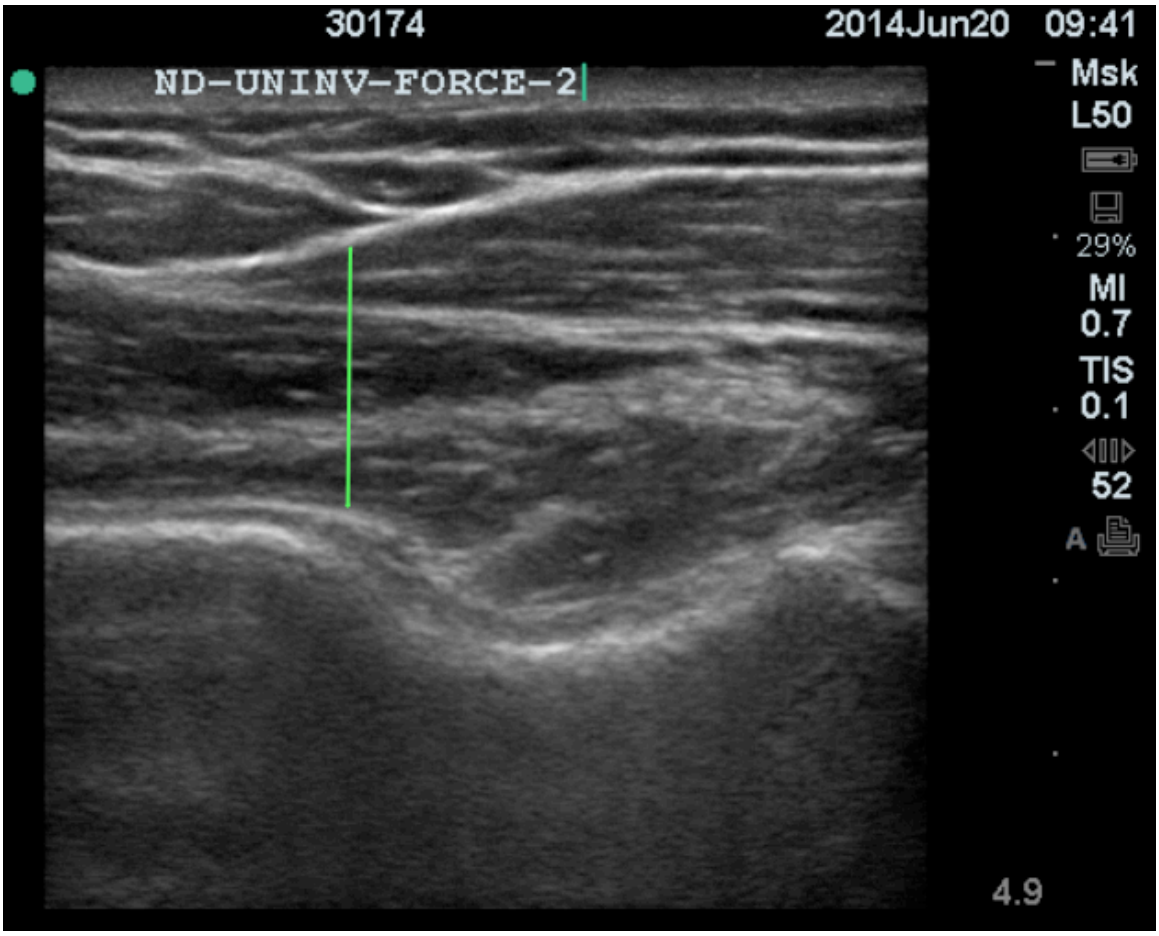

Figure 3.2: Compression force length measurement

Preliminary Study Results

Once data was obtained, the stress, strain, and stiffness for each trial was calculated. The mean and standard deviation of each was calculated, as shown in table 3.1. The stress and strain were plotted to produce a graph, Young's Modulus. Two separate graphs were produced: one for the healthy patients (dominant versus non-dominant) and one for post-operative patients (involved versus non-involved), as shown in figures 3.3 and 3.4. The calculated stiffness values were also graphed, shown in figures

3.5 and 3.6. For post-op patients, the external rotation and functional outcome scores, which range from 0-100 with 100 being fully functional, were recorded, as shown in table 3.2. The stress, strain, and stiffness for the post-op patients were then each graphed against the external rotation, as shown in figures 3.7-3.9.

		Strain (σ)		Stress (ε)		Stiffness	
		Mean	Std dev	Mean	Std dev	Mean	Std dev
Healthy patient 1	Dominant	0.16119 4853	0.03707 7643	55.6323 4091	16.1231 8326	8.90739 4047	1.89968 1064
	Non-dominant	0.10366 8075	0.04740 5893	35.4557 4681	15.9738 1086	9.42990 9537	0.55145 5885
Healthy Patient 2	Dominant	0.13368 5424	0.01255 9438	48.2523 7121	6.88539 8094	7.61849 658	0.57863 5833
	Non-dominant	0.19175 7092	0.02216 1055	64.601	10.5843 8253	9.26620 136	2.77483 1299
Healthy Patient 3	Dominant	0.14867 7212	0.03297 3723	52.1410 7576	1.09113 4087	11.0176 0849	1.56543 8252
	Non-dominant	0.14778 8249	0.11071 4768	122.773 6742	4.82289 1118	11.1924 8797	5.88064 0741
Healthy Patient 4	Dominant	0.12937 5908	0.10641 4672	59.6804 9242	8.24875 402	16.6094 1612	7.95279 3956
	Non-dominant	0.20016 4657	13.0427 0965	77.1401 8182	13.0427 0965	10.2690 7879	2.59823 3537
Post-op Patient 1	Involved	0.63365 1889	0.50142 7597	31.7449 2424	2.05273 1756	7.64246 5325	10.6887 9201
	Non-involved	0.11155 279	0.04671 9958	47.7762 1212	17.9030 5942	15.6879 3787	9.29193 6222
Post-op Patient 2	Involved	0.16325 3404	0.03628 4379	64.8390 9091	15.9809 2916	7.87477 8701	3.37474 8371
	Non-involved	0.20733 386	0.10037 2843	35.6337 1212	8.16578 1368	5.75633 7444	5.41392 7065
Post-op Patient 3	Involved	0.08570 1646	0.01774 1195	68.6484 8485	16.6343 8794	14.6770 6847	5.85445 7874
	Non-involved	0.14512 3425	0.08086 4795	56.8235 6061	0.49559 664	8.51200 732	4.65934 6869
Post-op Patient 4	Involved	0.11720 1619	0.05024 1965	37.0448 4848	7.59715 0314	9.95088 3545	5.81373 5105
	Non-involved	0.11720 1619	0.05024 1965	48.7298 4848	6.95190 9595	8.17124 838	4.07887 1634

Table 3.1: Statistical Analysis of Stain, Stress, and Stiffness

		External Rotation	Functional Outcome Score
Patient 1	Involved	10.9	96
	Non-involved	13.15	
Patient 2	Involved	21.4	91
	Non-involved	21.45	
Patient 3	Involved	20.65	96
	Non-involved	18.55	
Patient 4	Involved	11.65	93
	Non-involved	11.8	

Table 3.2: External Rotation and Functional Outcome for Post-op patients

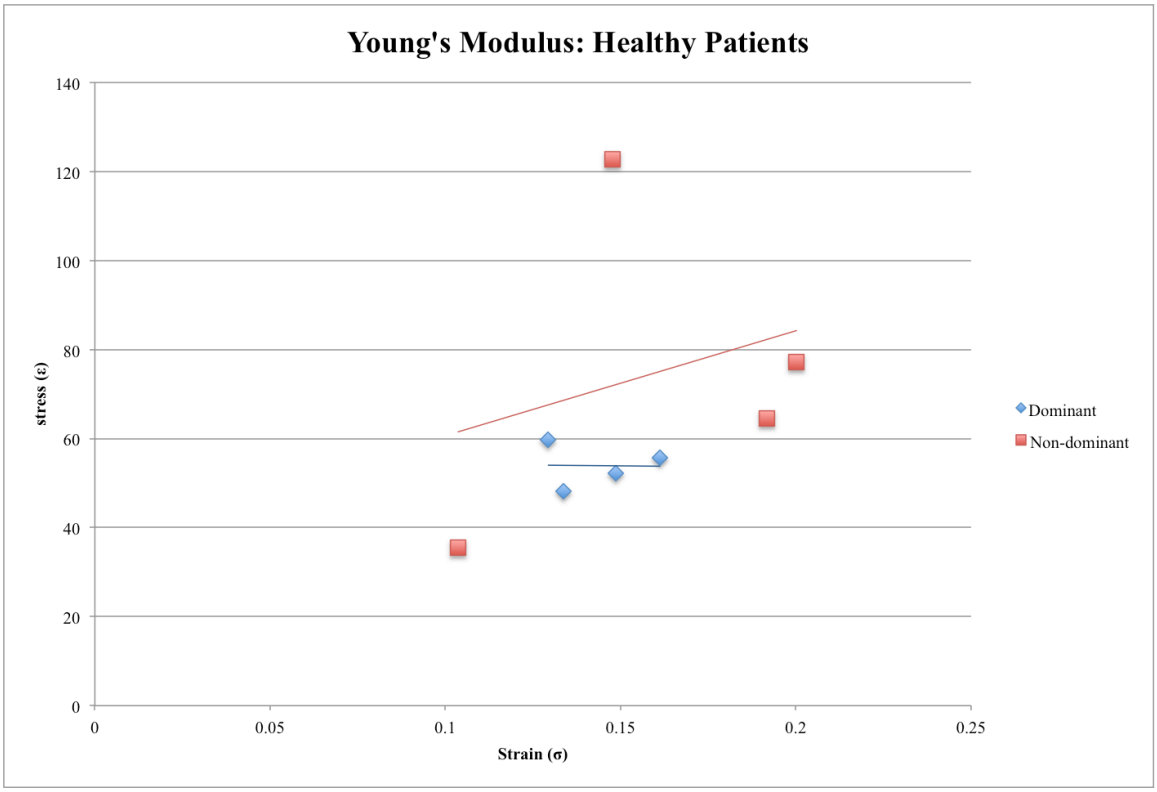

Figure 3.3: Stress versus Strain Curve: Healthy Patients

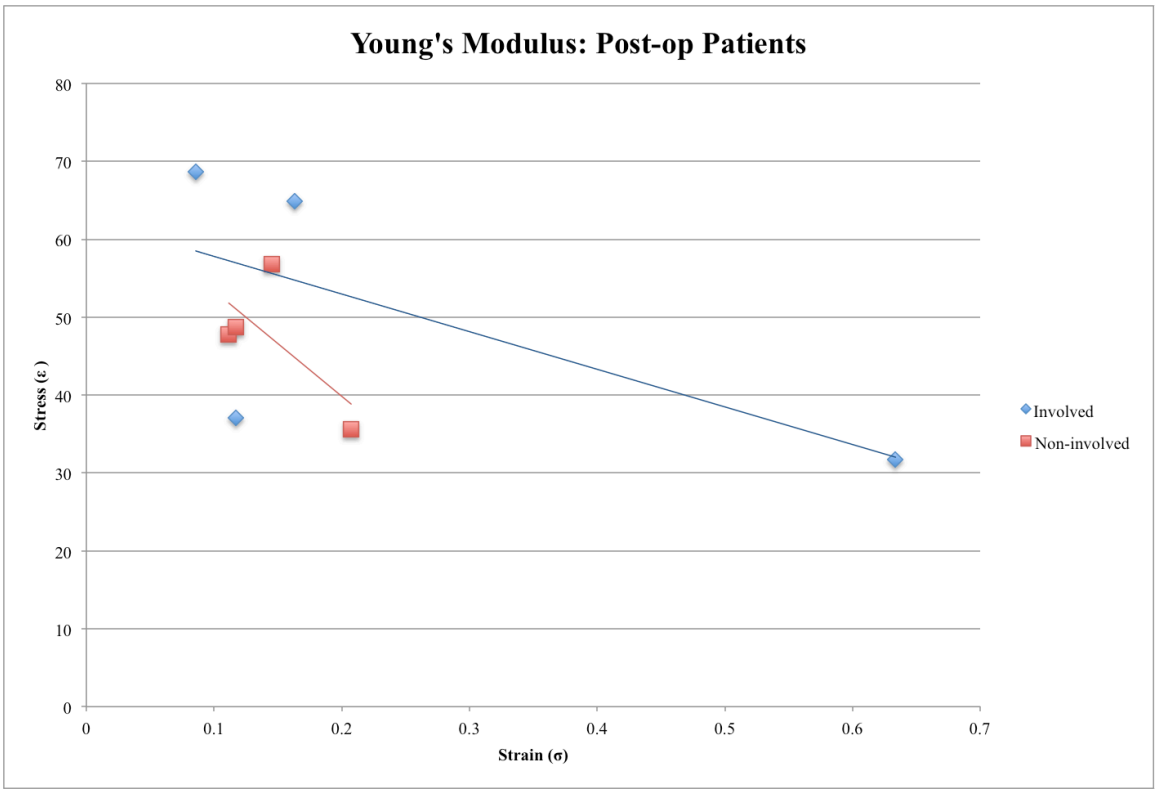

Figure 3.4: Stress versus Strain Curve: Post-operative Patients

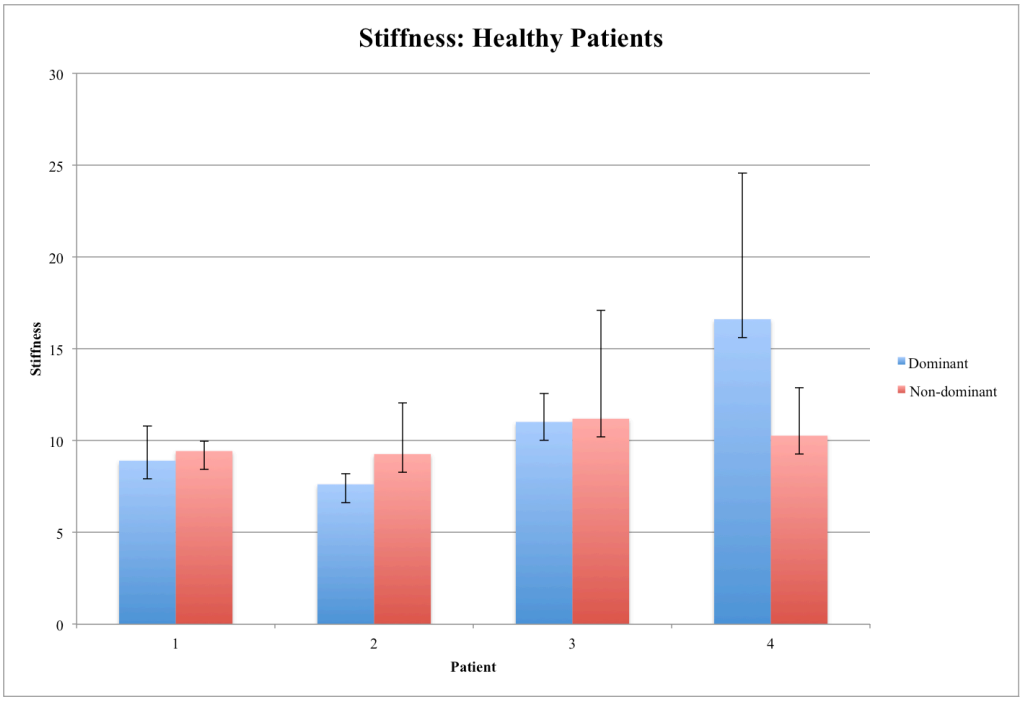

Figure 3.5: Healthy Patient Stiffness

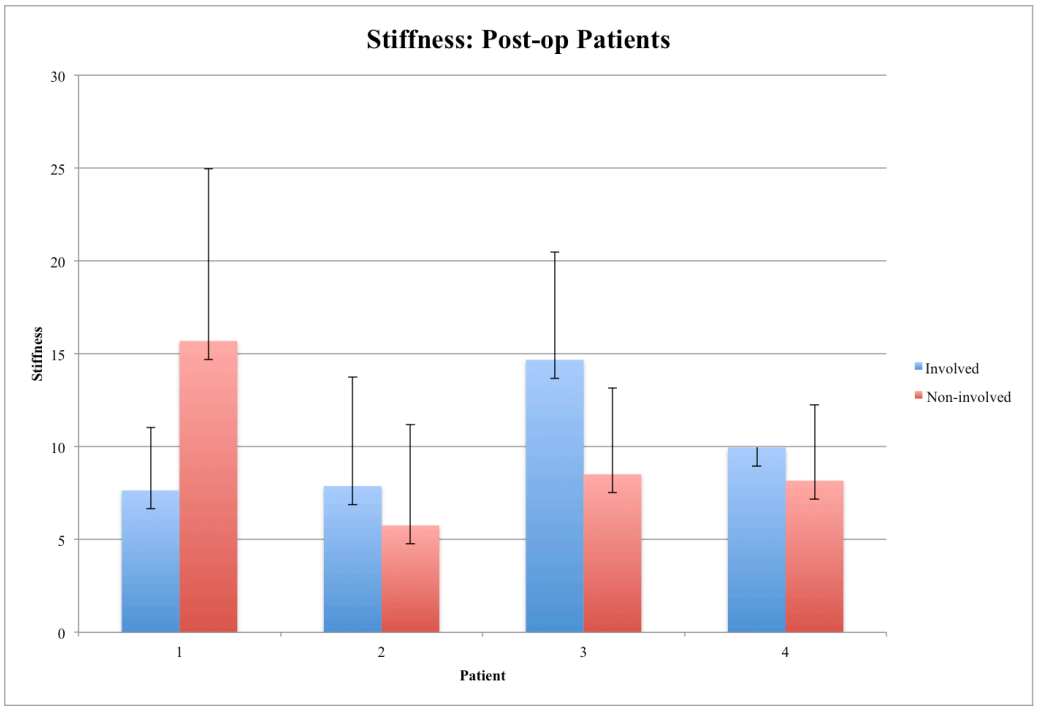

Figure 3.6: Post-op Patient Stiffness

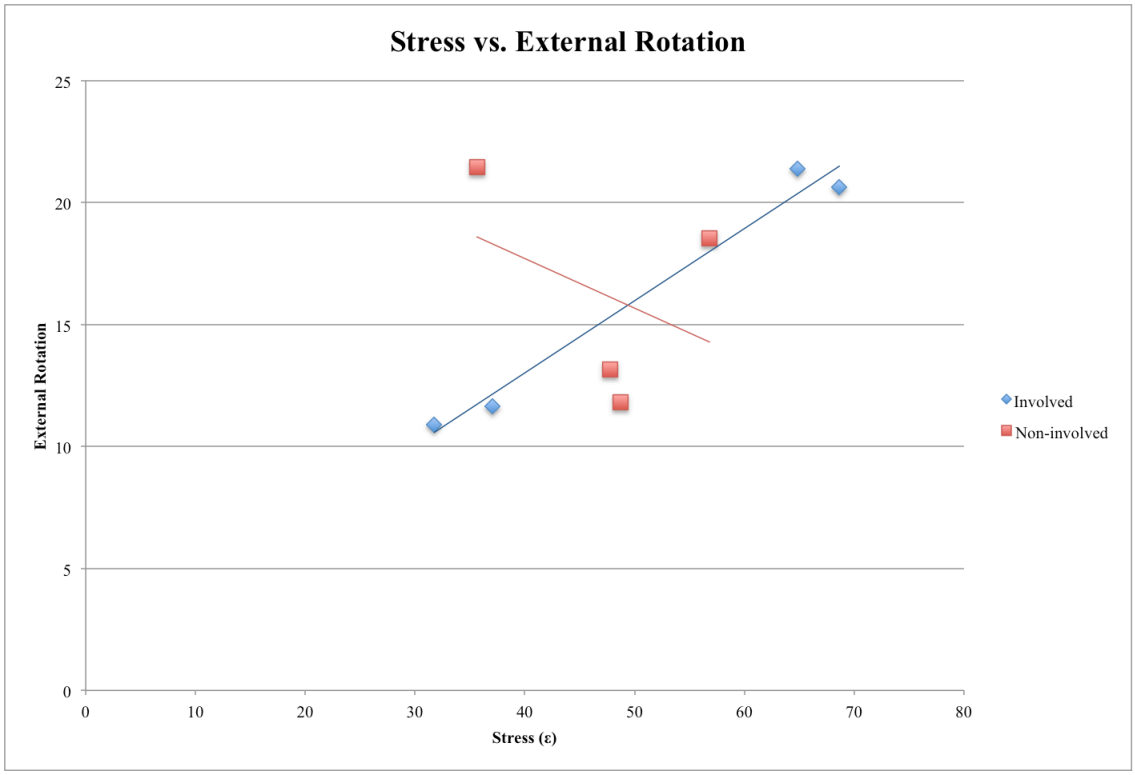

Figure 3.7: Stress vs. External Rotation for Post-op Patients

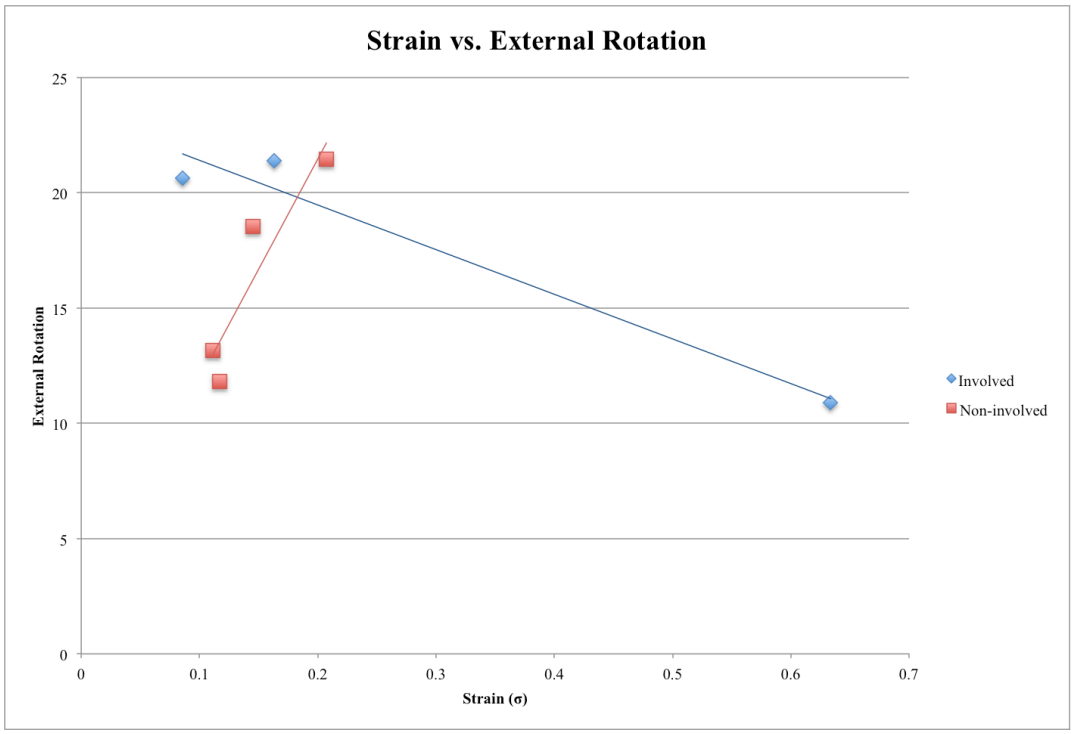

Figure 3.8: Strain vs. External Rotation for Post-op Patients

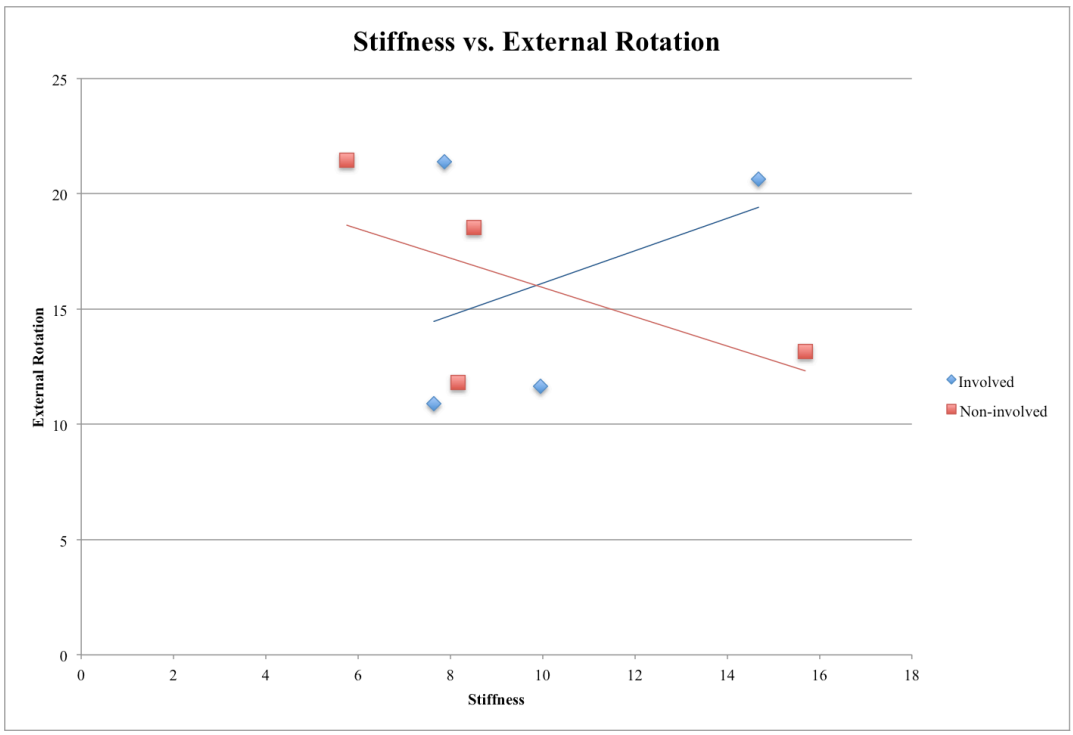

Figure 3.9: Stiffness vs External Rotation for Post-op Patients

For the healthy patients, when the dominant rotator cuff is under stress, the strain experienced by the tissue does not change. When the non-dominant rotator cuff is under stress, the strain experienced by the tissue increases, as shown in figure 3.3. For post-operative patients, an decrease in the strain experienced by the tissue was observed when the rotator cuff was put under stress in the involved and non-involved shoulder.

In the healthy patient sample, three patients had greater stiffness in their non-dominant shoulder, while the other had greater stiffness in their dominant. The one patient who had greater stiffness in the dominant shoulder was an overhead athlete, which could attribute to this difference. In the post-operative patients sample, three patients exhibited greater stiffness in their involved shoulder, while one patient exhibited greater stiffness in their non-involved.

For post-operative patients, when stress was compared to external rotation, increased external rotation was observed as stress increased in the involved shoulder, whereas decreased external rotation was seen when stress increased in the non-involved arm, as seen in figure 3.9. When compared to strain, decreased external rotation was observed as strain increased in the involved shoulder and increased external rotation was seen in the non-involved shoulder as strain increased, as seen in figure 3.8. With regards to stiffness, in the involved shoulder, increased external rotation was seen when stiffness increased. In the non-involved shoulder, deceased external rotation was observed when stiffness increased, as seen in figure 3.9.

CHAPTER FOUR

CONCLUSIONS AND DISCUSSION

Conclusion

The device produced is a significant improvement upon the previous iteration by improving several of the issues with the first iteration of the device. The issue of non-uniform force measurements was improved by incorporating a compression load cell sensor into the device, rather than the flex sensors used in the old device. This device is also smaller and lighter than the previous iteration, and is designed to better fit the contour of the human hand. This new design mitigates the learning curve involved in the use of the device that was experienced with the first iteration. This device also improves upon one of the complaints from clinicians about the previous iteration: the cables. By incorporating Bluetooth into the device, it does not have to be physically attached to a computer, allowing clinicians to use it more easily.

The study performed with the device not only provided preliminary results regarding the stress and strain experienced by the rotator cuff tissue in various patients, but also served to validate the utility of the device. The device was not only easy to use, but also produced conclusive results. An increase in the strain experienced by the tissue was observed as stress was applied in both the non-dominant shoulder in healthy patients and the involved shoulder in post-operative patients. Changes in the strain experienced by the tissue on the dominant side of healthy patients were not observed as stress was

applied. However, when stress was applied to the non-involved side of post-operative patients, a decreased amount of strain was observed.

Future Work

Although this device is a significant improvement upon the previous iteration, both in design and functioning, there is still room for improvements. Future plans include having a push button on the device that would allow for force data to be obtained in conjunction with the ultrasound image, to ensure both the quantitative data and qualitative images are obtained simultaneously with little effort. Ultimately, the goal with this device would be to record a video from the ultrasound, rather than just an image, in which the force measurements can be captured continuously. This will allow for the production of a stress versus strain curve, rather than just one value, in conjunction with a video of the compression of the tissue upon the administration of the force. This will allow for an even more complete diagnosis and monitoring of the injury.

Further work with this device can also be directed towards its use in anatomical areas other than the rotator cuff. For example, this device could be used on the Achilles tendon to aid in the diagnosis and monitoring of Achilles injuries, allowing for a more complete diagnosis than currently available. The device could also be used in the veterinary market. There are less diagnostic devices available for the animal model than the human model, and this device could be utilized to produce a more complete diagnosis for a range of injuries similar to those in humans.

WORKS CITED

1. Yamamoto A, Takagishi K, Osawa T, et al. Prevalence and risk factors of a rotator cuff tear in the general population. *J Shoulder Elbow Surg*. 2010;19(1):116-120. doi: 10.1016/j.jse.2009.04.006 [doi].

2. Minagawa H, Yamamoto N, Abe H, et al. Prevalence of symptomatic and asymptomatic rotator cuff tears in the general population: From mass-screening in one village. *J Orthop*. 2013;10(1):8-12. doi: 10.1016/j.jor.2013.01.008 [doi].

3. Bartolozzi A, Andreychik D, Ahmad S. Determinants of outcome in the treatment of rotator cuff disease. *Clin Orthop Relat Res*. 1994;(308)(308):90-97.

4. Milgrom C, Schaffler M, Gilbert S, van Holsbeeck M. Rotator-cuff changes in asymptomatic adults. the effect of age, hand dominance and gender. *J Bone Joint Surg Br*. 1995;77(2):296-298.

5. Gartsman GM, Brinker MR, Khan M, Karahan M. Self-assessment of general health status in patients with five common shoulder conditions. *J Shoulder Elbow Surg*. 1998;7(3):228-237.

6. Smith KL, Harryman DT,2nd, Antoniou J, Campbell B, Sidles JA, Matsen FA,3rd. A prospective, multipractice study of shoulder function and health status in patients with documented rotator cuff tears. *J Shoulder Elbow Surg*. 2000;9(5):395-402. doi: S1058-2746(00)04373-1 [pii].

7. Bytomski JR, Black D. Conservative treatment of rotator cuff injuries. *J Surg Orthop Adv*. 2006;15(3):126-131. doi: 15-3-1.pdf?T=open_article,943072 [pii].

8. MacDermid JC, Holtby R, Razmjou H, Bryant D, JOINTS Canada. All-arthroscopic versus mini-open repair of small or moderate-sized rotator cuff tears: A protocol for a randomized trial [NCT00128076. *BMC Musculoskelet Disord*. 2006;7:25. doi: 1471-2474-7-25 [pii].

9. Derwin KA, Baker AR, Iannotti JP, McCarron JA. Preclinical models for translating regenerative medicine therapies for rotator cuff repair. *Tissue Eng Part B Rev*. 2010;16(1):21-30. doi: 10.1089/ten.TEB.2009.0209 [doi].

10. Massimini DF, Boyer PJ, Papannagari R, Gill TJ, Warner JP, Li G. In-vivo glenohumeral translation and ligament elongation during abduction and abduction with internal and external rotation. *J Orthop Surg Res*. 2012;7:29-799X-7-29. doi: 10.1186/1749-799X-7-29 [doi].

11. Quilllen D, Wuchner M, Hatch R. Acute shoulder injuries. *American Family Physician*. 2004;70(10):1947-1954.

12. Fongeime A, Buss D, & Rolnick S. Management of shoulder impingement syndrome and rotator cuff tears. *Am Fam Physician*. 1998;57(4):667-674.

13. Blum K, Chen AL, Chen TJ, et al. Repetitive H-wave device stimulation and program induces significant increases in the range of motion of post operative rotator cuff reconstruction in a double-blinded randomized placebo controlled human study. *BMC Musculoskelet Disord*. 2009;10:132-2474-10-132. doi: 10.1186/1471-2474-10-132 [doi].

14. DEPALMA AF. Surgical anatomy of the rotator cuff and the natural history of degenerative periarthritis. *Surg Clin North Am*. 1963;43:1507-1520.

15. Post M, Silver R, Singh M. Rotator cuff tear: Diagnosis and treatment. *Clinical orthopaedics and related research*. 1983;173:78-91.

16. Escamilla RF, Yamashiro K, Paulos L, Andrews JR. Shoulder muscle activity and function in common shoulder rehabilitation exercises. *Sports Med*. 2009;39(8):663-685. doi: 10.2165/00007256-200939080-00004 [doi].

17. Neer CS,2nd. Impingement lesions. *Clin Orthop Relat Res*. 1983;(173)(173):70-77.

18. Reilly P, Macleod I, Macfarlane R, Windley J, Emery RJ. Dead men and radiologists don't lie: A review of cadaveric and radiological studies of rotator cuff tear prevalence. *Ann R Coll Surg Engl*. 2006;88(2):116-121. doi: 10.1308/003588406X94968 [doi].

19. Jerosch J, Muller T, Castro WH. The incidence of rotator cuff rupture. an anatomic study. *Acta Orthop Belg*. 1991;57(2):124-129.

20. Matthews TJ, Hand GC, Rees JL, Athanasou NA, Carr AJ. Pathology of the torn rotator cuff tendon. reduction in potential for repair as tear size increases. *J Bone Joint Surg Br*. 2006;88(4):489-495. doi: 88-B/4/489 [pii].

21. Yamanaka K, Matsumoto T. The joint side tear of the rotator cuff. A followup study by arthrography. *Clin Orthop Relat Res*. 1994;(304)(304):68-73.

22. Yu TY, Tsai WC, Cheng JW, Yang YM, Liang FC, Chen CH. The effects of aging on quantitative sonographic features of rotator cuff tendons. *J Clin Ultrasound*. 2012;40(8):471-478. doi: 10.1002/jcu.21919 [doi].

23. Fuchs S, Chylarecki C, Langenbrinck A. Incidence and symptoms of clinically manifest rotator cuff lesions. *Int J Sports Med*. 1999;20(3):201-205. doi: 10.1055/s-2007-971118 [doi].

24. Sher JS, Uribe JW, Posada A, Murphy BJ, Zlatkin MB. Abnormal findings on magnetic resonance images of asymptomatic shoulders. *J Bone Joint Surg Am*. 1995;77(1):10-15.

25. Yamaguchi K, Tetro AM, Blam O, Evanoff BA, Teefey SA, Middleton WD. Natural history of asymptomatic rotator cuff tears: A longitudinal analysis of asymptomatic tears detected sonographically. *J Shoulder Elbow Surg*. 2001;10(3):199-203. doi: S1058-2746(01)10756-1 [pii].

26. Lehman C, Cuomo F, Kummer FJ, Zuckerman JD. The incidence of full thickness rotator cuff tears in a large cadaveric population. *Bull Hosp Jt Dis*. 1995;54(1):30-31.

27. Yang S, Park H, Flores S, et al. Biomechanical analysis of bursal-sided partial thickness rotator cuff tears. *Journal of Shoulder and Elbow Surgery*. 2009;18(3):379-385. doi: http://dx.doi.org/10.1016/j.jse.2008.12.011.

28. Gimbel JA, Van Kleunen JP, Mehta S, Perry SM, Williams GR, Soslowsky LJ. Supraspinatus tendon organizational and mechanical properties in a chronic rotator cuff tear animal model. *J Biomech*. 2004;37(5):739-749. doi: 10.1016/j.jbiomech.2003.09.019 [doi].

29. Zingg PO, Jost B, Sukthankar A, Buhler M, Pfirrmann CW, Gerber C. Clinical and structural outcomes of nonoperative management of massive rotator cuff tears. *J Bone Joint Surg Am*. 2007;89(9):1928-1934. doi: 89/9/1928 [pii].

30. Gerber C, Schneeberger AG, Hoppeler H, Meyer DC. Correlation of atrophy and fatty infiltration on strength and integrity of rotator cuff repairs: A study in thirteen patients. *J Shoulder Elbow Surg*. 2007;16(6):691-696. doi: S1058-2746(07)00333-3 [pii].

31. Vitale MA, Vitale MG, Zivin JG, Braman JP, Bigliani LU, Flatow EL. Rotator cuff repair: An analysis of utility scores and cost-effectiveness. *J Shoulder Elbow Surg*. 2007;16(2):181-187. doi: S1058-2746(06)00321-1 [pii].

32. Silverstein B. KJ. Work-related musculoskeletal disorders of the neck, back, and upper extremity in washington state, 1992-2000. . 2002;40-6-2002.

33. Herberts P, Kadefors R, Hogfors C, Sigholm G. Shoulder pain and heavy manual labor. *Clin Orthop Relat Res*. 1984;(191)(191):166-178.

34. Ebell MH. Point of care guides: Diagnosing rotator cuff tears. *Am Fam Physician*. 2005;71(8):1587.

35. Jain NB, Yamaguchi K. History and physical examination provide little guidance on diagnosis of rotator cuff tears. *Evid Based Med*. 2014;19(3):108-2013-101593. Epub 2013 Dec 17. doi: 10.1136/eb-2013-101593 [doi].

36. Farshad-Amacker NA, Jain Palrecha S, Farshad M. The primer for sports medicine professionals on imaging: The shoulder. *Sports Health*. 2013;5(1):50-77. doi: 10.1177/1941738112468265 [doi].

37. Reinus WR, Shady KL, Mirowitz SA, Totty WG. MR diagnosis of rotator cuff tears of the shoulder: Value of using T2-weighted fat-saturated images. *AJR Am J Roentgenol*. 1995;164(6):1451-1455. doi: 10.2214/ajr.164.6.7754891 [doi].

38. Bey MJ, Derwin KA. Measurement of in vivo tendon function. *J Shoulder Elbow Surg*. 2012;21(2):149-157. doi: 10.1016/j.jse.2011.10.023 [doi].

39. Al-Shawi A, Badge R, Bunker T. The detection of full thickness rotator cuff tears using ultrasound. *J Bone Joint Surg Br*. 2008;90(7):889-892. doi: 10.1302/0301-620X.90B7.20481 [doi].

40. Read JW, Perko M. Shoulder ultrasound: Diagnostic accuracy for impingement syndrome, rotator cuff tear, and biceps tendon pathology. *J Shoulder Elbow Surg*. 1998;7(3):264-271.

41. Farin PU, Kaukanen E, Jaroma H, Vaatainen U, Miettinen H, Soimakallio S. Site and size of rotator-cuff tear. findings at ultrasound, double-contrast arthrography, and computed tomography arthrography with surgical correlation. *Invest Radiol*. 1996;31(7):387-394.

42. Burk DL,Jr, Karasick D, Kurtz AB, et al. Rotator cuff tears: Prospective comparison of MR imaging with arthrography, sonography, and surgery. *AJR Am J Roentgenol*. 1989;153(1):87-92. doi: 10.2214/ajr.153.1.87 [doi].

43. Swen WA, Jacobs JW, Algra PR, et al. Sonography and magnetic resonance imaging equivalent for the assessment of full-thickness rotator cuff tears. *Arthritis Rheum*. 1999;42(10):2231-2238. doi: 10.1002/1529-0131(199910)42:10<2231::AID-ANR27>3.0.CO;2-Z [doi].

44. de Jesus JO, Parker L, Frangos AJ, Nazarian LN. Accuracy of MRI, MR arthrography, and ultrasound in the diagnosis of rotator cuff tears: A meta-analysis. *AJR Am J Roentgenol*. 2009;192(6):1701-1707. doi: 10.2214/AJR.08.1241 [doi].

45. Bachmann GF, Melzer C, Heinrichs CM, Mohring B, Rominger MB. Diagnosis of rotator cuff lesions: Comparison of US and MRI on 38 joint specimens. *Eur Radiol*. 1997;7(2):192-197.

46. Zhang C, Guo L, An N, Liu GH, Zhu YT, Fan LJ. Application value of high-frequency ultrasound on the diagnosis of rotator cuff tears. *Zhongguo Gu Shang*. 2013;26(9):784-786.

47. Rutten MJ, Spaargaren GJ, van Loon T, de Waal Malefijt MC, Kiemeney LA, Jager GJ. Detection of rotator cuff tears: The value of MRI following ultrasound. *Eur Radiol*. 2010;20(2):450-457. doi: 10.1007/s00330-009-1561-9 [doi].

48. Bull AM, Reilly P, Wallace AL, Amis AA, Emery RJ. A novel technique to measure active tendon forces: Application to the subscapularis tendon. *Knee Surg Sports Traumatol Arthrosc*. 2005;13(2):145-150. doi: 10.1007/s00167-004-0556-y [doi].

49. Reilly P, Bull AM, Amis AA, Wallace AL, Emery RJ. Arthroscopically insertable force probes in the rotator cuff in vivo. *Arthroscopy*. 2003;19(2):E8. doi: 10.1053/jars.2003.50050 [doi].

50. Kim YS, Kim JM, Bigliani LU, Kim HJ, Jung HW. In vivo strain analysis of the intact supraspinatus tendon by ultrasound speckles tracking imaging. *J Orthop Res*. 2011;29(12):1931-1937. doi: 10.1002/jor.21470 [doi].

51. Arampatzis A, Stafilidis S, DeMonte G, Karamanidis K, Morey-Klapsing G, Bruggemann GP. Strain and elongation of the human gastrocnemius tendon and aponeurosis during maximal plantarflexion effort. *J Biomech*. 2005;38(4):833-841. doi: S0021929004002398 [pii].

52. Arampatzis A, Peper A, Bierbaum S, Albracht K. Plasticity of human achilles tendon mechanical and morphological properties in response to cyclic strain. *J Biomech*. 2010;43(16):3073-3079. doi: 10.1016/j.jbiomech.2010.08.014 [doi].

53. Gerus P, Rao G, Berton E. A method to characterize in vivo tendon force-strain relationship by combining ultrasonography, motion capture and loading rates. *J Biomech*. 2011;44(12):2333-2336. doi: 10.1016/j.jbiomech.2011.05.021 [doi].

54. Farron J, Varghese T, Thelen DG. Measurement of tendon strain during muscle twitch contractions using ultrasound elastography. *IEEE Trans Ultrason Ferroelectr Freq Control*. 2009;56(1):27-35. doi: 10.1109/TUFFC.2009.1002 [doi].

55. Maganaris CN, Paul JP. Load-elongation characteristics of in vivo human tendon and aponeurosis. *J Exp Biol*. 2000;203(Pt 4):751-756.

56. Hansen P, Bojsen-Moller J, Aagaard P, Kjaer M, Magnusson SP. Mechanical properties of the human patellar tendon, in vivo. *Clin Biomech (Bristol, Avon)*. 2006;21(1):54-58. doi: S0268-0033(05)00177-4 [pii].

57. O'Brien TD, Reeves ND, Baltzopoulos V, Jones DA, Maganaris CN. Mechanical properties of the patellar tendon in adults and children. *J Biomech*. 2010;43(6):1190-1195. doi: 10.1016/j.jbiomech.2009.11.028 [doi].

58. Trent E, Bailey L, Meflah F, et al. Assessment and characterization of in situ rotator cuff biomechanics. *Medical Imaging 2013: Biomedical Applications in Molecular, Structural, and Functional Imaging*. 2013;8672.

59. sparkfun. Fio v3- ATmega32U4. https://www.sparkfun.com/products/11520. Accessed 5/30, 2014.